A Surface Science Study of Model Catalysts. 1. Quantitative Surface Analysis of Wet-Chemically Prepared Cu/SiO_2 Model Catalysts

L. C. A. van den Oetelaar,† A. Partridge, P. J. A. Stapel, C. F. J. Flipse, and H. H. Brongersma*

Faculty of Physics and Schuit Institute of Catalysis, Eindhoven University of Technology, P.O. Box 513, 5600 MB Eindhoven, The Netherlands

Received: July 13, 1998

Cu/SiO_2 model catalysts containing nanometer-sized Cu particles on a flat silica model support were wet-chemically prepared and characterized in detail by a variety of surface science techniques. The particle size and shape, particle number density, metal surface coverage, total metal loading, and oxidation state of the particles were determined by ultrahigh vacuum atomic force microscopy, electron microscopy, low-energy ion scattering, Rutherford backscattering spectrometry, and X-ray photoelectron spectroscopy. Deposition of a Cu precursor on a flat Si wafer with a SiO_2 top layer by spin-coating was followed by calcination in air at 450 °C. This preparation method produces both homogeneously distributed hemispherical CuO particles with an average height of 8 nm and highly dispersed oxidic Cu species. Subsequent reduction in hydrogen at 250 °C results in metallic and more rounded Cu particles with an average height of 8 nm.

1. Introduction

Catalysis research aims at the understanding of the relations between the preparation, properties, and performance of a catalyst. A heterogeneous metal catalyst is a material with a complex structure and these relations cannot be established easily. One approach to facilitate catalysis research is to use model catalysts in experimental studies of surface and interface phenomena of heterogeneous catalysts.

Different types of model catalysts exist. The most simple and best defined model catalyst is a single crystal. More complex, but also more realistic (regarding the structure), are supported model catalysts. They can be prepared by deposition via metal evaporation, wet-chemical methods, chemical vapor deposition, or lithographic procedures on various types of model supports.[1] The appropriate model system is selected and prepared depending on the topic(s) of interest. To obtain relevant information about surface and interface phenomena of technically important catalysts, one should strive both for detailed characterization of the properties and for testing of the model catalyst in a catalytic reaction.

This paper describes the preparation and characterization of Cu/SiO_2 model catalysts. The Cu/SiO_2 model catalysts contain nanometer-sized Cu particles on a flat silica model support. They are prepared in a similar way as used for technically important metal catalysts on porous supports, namely by wet-chemical deposition of a Cu precursor, followed by calcination and reduction to produce metallic Cu particles. The wet-chemical deposition onto flat SiO_2 supports was carried out using the spin-coating technique. This technique mimics the impregnation step in the preparation of porous metal catalysts. Spin-coating was introduced as a deposition method to prepare model metal catalysts by Kuipers et al.,[2−4] and was further developed and used by others.[5−9] Properties such as the particle size and shape, particle number density, metal surface coverage, total metal loading, and oxidation state of the particles were determined, using a variety of characterization techniques as summarized in the experimental section.

There are several applications of supported Cu catalysts. Silica-supported Cu can be used as a catalyst for various reactions, such as the water−gas shift reaction, methanol steam reforming, (de)hydrogenation reactions, and hydrogenolysis of esters.[10,11] Supported Cu−ZnO catalysts are industrially applied in methanol synthesis. After more than 25 years of research, the catalytically active site(s) of this catalyst still is not determined precisely, but the important role of Cu (in interaction with ZnO) has been recognized.[12,13] The Cu/SiO_2 system has been used as a reference system in such studies.[14−16]

The interaction of the metal particles with the support determines several processes, such as sintering and encapsulation of metal particles by the support, which influence the catalytic activity and selectivity. Therefore, the metal−support interactions in Cu/SiO_2 model catalysts will be discussed in an accompanying paper[17] after a detailed study of the structure of the Cu model catalyst during preparation is presented here.

2. Experimental Section

2.1. Spin-Coating of a Cu Precursor onto SiO_2 Substrates. To obtain realistic Cu/SiO_2 model catalysts, we chose to use spin-coating for deposition of a Cu precursor on a SiO_2 model support. Solutions of $Cu(CH_3COO)_2{\cdot}H_2O$ ($Cu(acetate)_2$) in ethanol or 1-butanol were used to produce the small copper particles, following the procedure outlined in refs 8 and 9. Butanol was later used in preference to ethanol as a solvent because the use of ethanol tended to produce inhomogeneous particle distributions, which can be attributed to water condensation from the atmosphere during spin-coating or to the relatively high water content of ethanol itself.[8,9] Because of the poor wettability of the substrate by water, liquid films containing much water will break up during spin-coating.[4] Water is less soluble in butanol than in ethanol and the lower rate of evaporation of butanol may reduce water condensation as a result of surface supercooling. Spin-coating was always performed in a glove box under dry atmospheric or inert nitrogen conditions to minimize water condensation. Another way to

* Corresponding author. Fax: +31-40-2453587. E-mail: hidde@surf.phys.tue.nl.

† Present address: Akzo Nobel Central Research, Department of Applied Physics (RGC), P.O. Box 9300, 6800 SB Arnhem, The Netherlands.

10.1021/jp982998e CCC: $15.00
Published on Web 11/04/1998

avoid the problem mentioned above is to hydrolyze the support surface prior to spin-coating to improve the wettability of the support by water.[4]

The substrates used to support the deposited particles were Si(100) wafers, which had been oxidized in air at 500 °C for 24 h to produce a 5 nm oxide layer. This treatment leads to a SiO_2 surface which is acceptable as a model of a silica support[1,18] based on the Si 2p binding energy of the oxide layer (from X-ray photoelectron spectroscopy (XPS)),[19,20] although note that these surfaces will not be fully hydroxylated. The amount of OH groups on the SiO_2 layer prepared by dry oxidation at 500 °C is about 2 OH groups/nm^2.[21−24] Prior to deposition, substrates were spin-cleaned in proanalysis alcohol.

For the samples discussed in this paper, the Cu deposition was carried out by spin-coating a 0.01 M solution of Cu(acetate)$_2$ in 1-butanol onto substrates with a thin (5 nm) SiO_2 top layer at a spin frequency of 5000 rpm. Following deposition, the Cu acetate complexes were transformed into CuO particles by calcination in air at 450 °C for 4 h at a ramp rate of 300 °C/h.

2.2. Ultrahigh Vacuum Atomic Force Microscopy (UHV-AFM) and Electron Microscopy. AFM measurements were performed with an Omicron UHV-AFM, using cantilevers with integrated Si_3N_4 pyramidal tips.[25] All of the measurements were performed in contact mode, applying a low normal force, typically of the order of 1 nN. After transfer to the AFM, the samples received a short recalcination to burn off surface carbon contaminations (50 mbar O_2 at 300 °C for 30 min). To obtain metallic Cu particles, the samples were then reduced in a static hydrogen atmosphere (50 mbar H_2 at 250 °C for 1 h), the hydrogen being periodically refreshed during reduction. These procedures were carried out in a prechamber of the AFM setup. This means that the samples were not exposed to ambient conditions between treatment steps so that AFM analysis of the samples between steps could be performed. The dispersion of the copper particles was studied as a function of the oxidation and reduction procedure. Accurate quantitative information about the particle height and particle number density can be obtained with AFM. Because of the tip−particle convolution, the particle diameter cannot be accurately determined.[8]

Some samples were also investigated using electron microscopy. High-resolution scanning electron microscopy (HRSEM) measurements were done at the Shell Research and Technology Centre in Amsterdam (SRTCA). In addition to the 3D information of the sample morphology obtained with AFM, HRSEM gives a 2D top view projection of the sample surface and quantitative information about the particle diameter. AFM and electron microscopy can complement each other to yield accurate information about the particle shape of nanoscale systems.[26]

2.3. Low-Energy Ion Scattering (LEIS) and XPS. The samples were also analyzed by LEIS to determine the Cu surface coverage, using the NODUS setup described in ref 27. LEIS was performed using 3 keV $^4He^+$ ions (scattering angle of 142°) with a beam current of 30 nA, using a typical ion dose of 2.1 $\times$ 10^{14} ions/cm^2 during one measurement. The Cu signal from the samples was calibrated by a reference sample of clean polycrystalline pure Cu. The Cu/SiO_2 samples were prepared in situ prior to analysis, following the procedure outlined in section 2.2.

The chemical state of the copper particles after oxidation and reduction was checked by a VG ESCALAB 200 XPS system, using a standard Al Kα source. In this case, the samples were prepared in the prechamber of the NODUS prior to transportation of the samples to a nitrogen glove box using a vacuum suitcase. The samples were then transferred to another vacuum suitcase compatible with the XPS system for analysis. It became evident that this transfer procedure did not affect the oxidation state of the copper particles even though some carbon contamination did occur during transportation.

TABLE 1: Results from RBS and AFM Measurements of Three Cu Model Catalysts (Samples I, II, III) Prepared in the Same Way[a]

	RBS	AFM	
	Cu loading l (10^{15} at/cm^2)	particle density n (10^{10} part/cm^2)	particle height h (nm)
I	1.36 ± 0.1	2.0 ± 0.5	8 ± 2
II	1.55 ± 0.1	2.3 ± 0.5	8 ± 2
III	1.85 ± 0.1	1.8 ± 0.5	8 ± 2

[a] No difference (within experimental error) was observed between calcined and reduced model catalysts.

2.4. Rutherford Backscattering Spectrometry (RBS). Metal loadings following spin-coating, calcination, and reduction were quantified with RBS using 4 MeV He^+ ions from the AVF-cyclotron at the Eindhoven University of Technology.[28] The beamguiding system was operated in the dispersive mode resulting in $\Delta E/E = 3 \times 10^{-3}$. Scattering experiments were carried out in a standard high-vacuum scattering chamber (with a pressure of about 1×10^{-5} mbar), and the angle of the incoming beam with the sample surface normal was 5°. Scattered particles were detected with a standard passivated implanted planar silicon (PIPS) detector which was positioned at a scattering angle of 165° with respect to the direction of the incoming beam. The measured overall energy resolution (full width at half maximum) was found to be 18 keV, sufficient to identify the ^{63}Cu and ^{65}Cu isotopes separately.

3. Results and Discussion

3.1. Cu Deposition by Spin-Coating. The composition and structure of a model catalyst is influenced by several parameters in the spin-coating procedure, analogous to the preparation of technical catalysts by impregnation. A number of studies were performed to determine these parameters and their influence on the properties of the model catalyst to enable the controlled preparation of model catalysts. In the original work of Kuipers et al.,[2] the influence of the solute concentration and spin frequency on the particle size and number density were discussed. A decrease of the solute concentration and an increase of the spin frequency result in a decrease of particle size and increase of particle number density, but independent control of these two properties is not possible. In addition, atmospheric properties (humidity), solvent properties (evaporation rate), chemistry of the solute, and the condition of the substrate were found to influence the properties of the model catalyst.[4,5,9,29,30] Whether isolated particles or thin layers are deposited after spin-coating depends on the metal precursor. Cu(acetate)$_2$ is deposited as a thin layer, while Cu(NO$_3$)$_2$ is deposited as particles after spin-coating (with 5000 rpm) of the metal precursor dissolved in ethanol. The difference is attributed to a larger region of metastability in the solvent for the acetate precursor than for the nitrate precursor.[9]

The metal loading can be predicted from a hydrodynamic model of spin-coating and can be checked by RBS measurements. A good agreement between theory and experiment was found.[5,8] In Table 1, the Cu loadings (l) as determined by RBS of the samples studied in this paper are shown. The RBS measurements are carried out after the reduction step, and a typical RBS spectrum of a Cu/SiO_2 model catalyst is shown in Figure 1. Because no loss of Cu occurs during calcination and

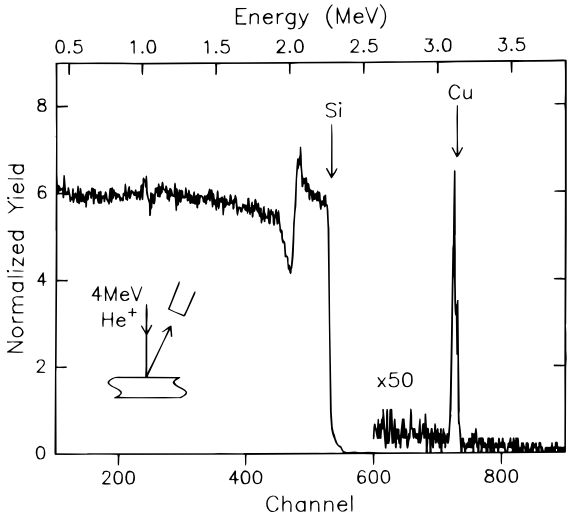

Figure 1. A typical RBS spectrum of a Cu/SiO_2 model catalyst, using 4 MeV He^+ ions.

reduction under the conditions used here (checked by RBS), the measured Cu loading also represents the amount of Cu deposited by spin-coating. The samples presented in Table 1 are all prepared in the same way. As shown in ref 8, a Cu loading of 1.5×10^{15} at/cm^2 is predicted on the basis of the spin-coating theory, which takes into account the solute concentration and spin frequency. This is in good agreement with the experimental values of the Cu loading in Table 1.

3.2. Calcination and Reduction. On calcination, the deposited Cu acetate film will break up and form CuO particles. It is expected that the heating procedure will affect the particle formation. After slow heating to 450 °C, at a ramp rate of 50 °C/h, the particle size and distribution was not very reproducible and only a small number of particles were observed by AFM.[9] Reproducible results were found when a high ramp rate of 300 °C/h was used. During heating, Cu acetate is mobile in the deposited layer and can cluster prior to dissociation. Temperatures in excess of 250 °C are required to produce appreciable rates of Cu acetate dissociation and oxidation. On rapid heating, the time available for surface diffusion of Cu acetate is restricted, because the temperature at which Cu acetate dissociates and oxidizes is quickly attained.

After calcination at 450 °C in air, the chemical composition of the particles was determined by XPS. The position of the Cu $2p_{3/2}$ peak was at 934.1 eV and the Cu LMM peak was at 569.4 eV, consistent with CuO.[31,32] The given binding energies were corrected for charging of the sample (+1.2 eV) by using the C ls binding energy which was expected to be at 284.6 eV. The Cu^{2+} satellites (from shake-up transitions) are clearly visible in the Cu 2p XPS spectrum (see Figure 2a). The CuO particles can be converted into metallic Cu particles by reduction in hydrogen at 250 °C. After reduction in hydrogen, the Cu^{2+} satellites disappeared, the Cu $2p_{3/2}$ peak shifted to 932.5 eV, and the Cu LMM shifted to 568.2 eV (see Figure 2b), consistent with the formation of Cu^0.[31,32]

The calcination and reduction steps are not only important for the conversion of the deposited Cu precursor into catalytically active Cu sites, but also for anchoring of the particles to the support. The anchoring of the Cu particles to the SiO_2 substrate is assumed to occur during the calcination step and will be discussed in more detail in an accompanying paper.[17] Anchoring by a reduction step was observed in the case of Rh/SiO_2 model catalysts[9] in which the Rh particles are only weakly bonded to the SiO_2 support directly after spin-coating of a $RhCl_3$ precursor in ethanol onto this support, because the AFM tip can readily move these particles around. However, after reduction of the particles in hydrogen at 200 °C, the particles can no longer be swept or destroyed by the AFM tip.

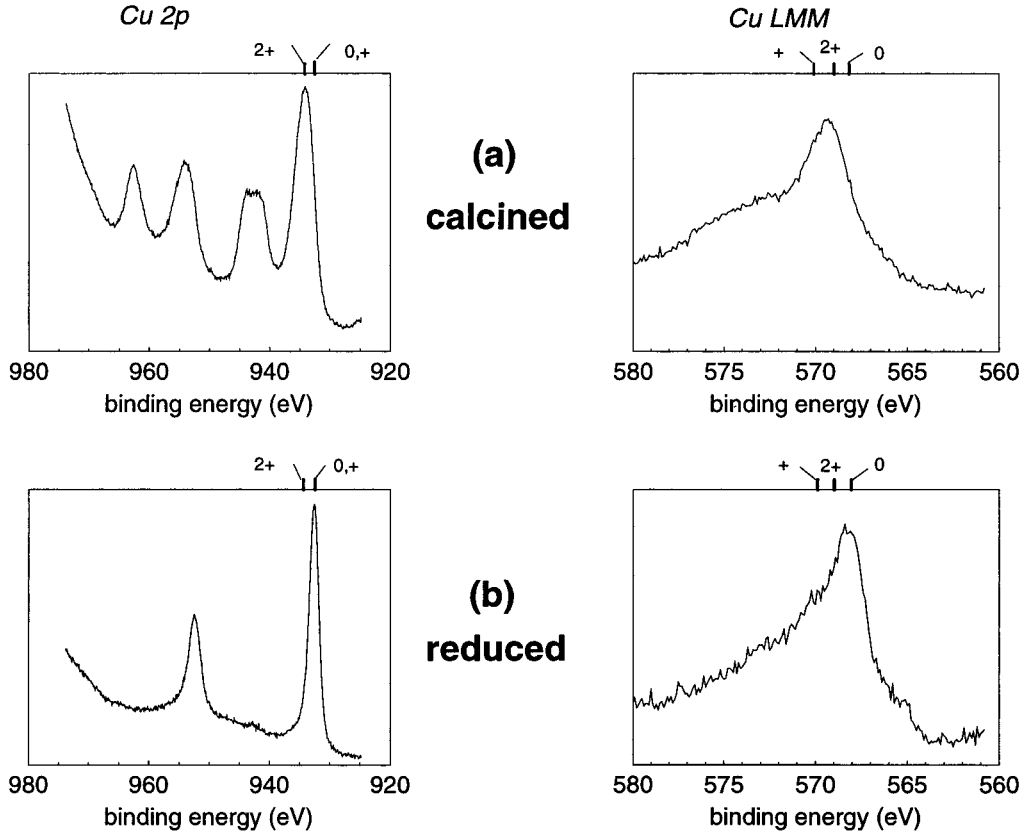

Figure 2. XPS spectra of a Cu/SiO_2 model catalyst (a) after calcination (Cu oxidation state: 2+) and (b) after reduction (Cu oxidation state: 0).

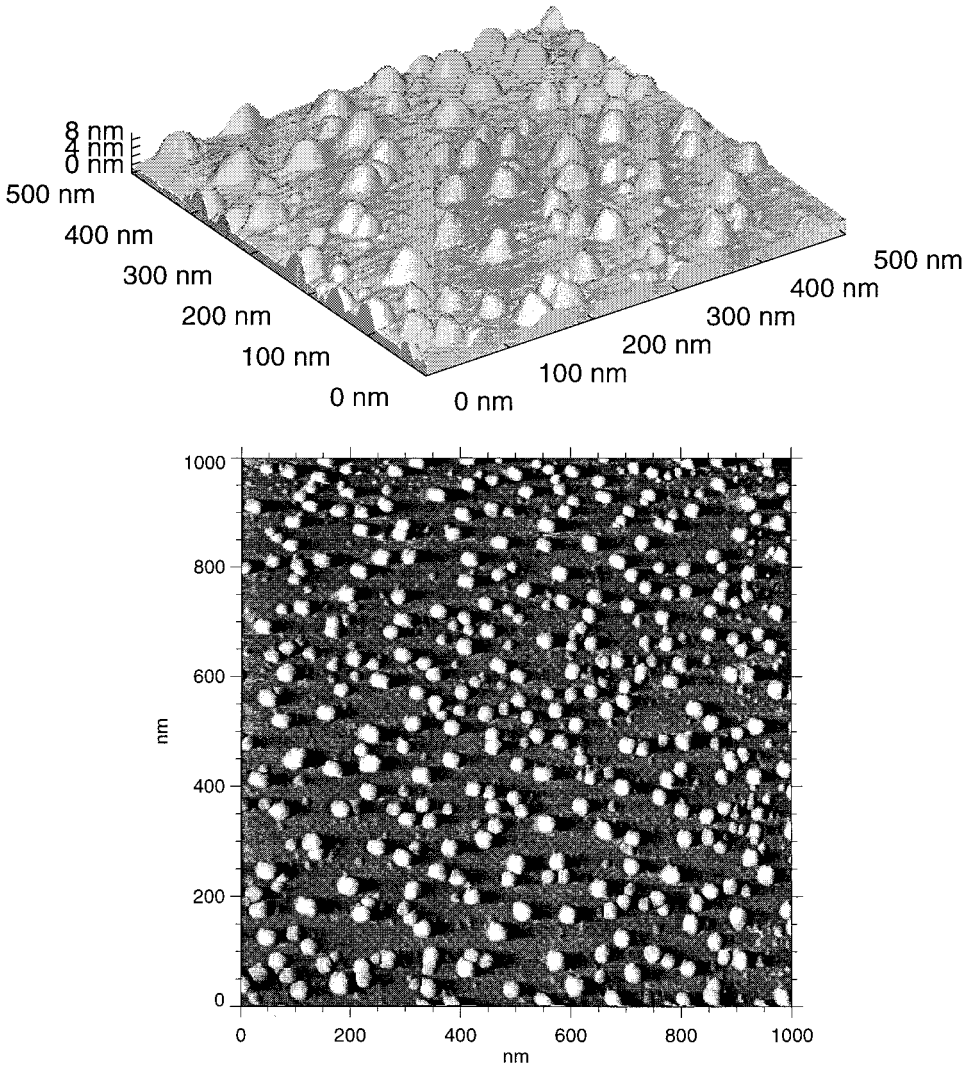

Figure 3. UHV-AFM images (measured in contact mode) of a Cu/SiO_2 model catalyst: (a) 3D image obtained in topographical mode and (b) 2D image obtained in frictional mode.

3.3. Morphology of the Cu/SiO_2 Model Catalyst. The particle size and number density of the metal component of a catalyst can have a significant influence on the catalytic performance.[33] For a model catalyst with a flat substrate these properties can be studied in detail with scanning probe and electron microscopy.

Figure 3a shows a topographical picture of the surface of the Cu/SiO_2 model catalyst obtained by UHV-AFM after calcination. The 2D top view projection in Figure 3b, measured in frictional mode, clearly shows the homogeneous distribution of CuO particles over the SiO_2 surface. Because of the tip−particle convolution, the real particle diameter is much smaller than suggested by Figure 3b.[8] Because deconvolution is not straightforward, only the particle height *h* and number density *n* were determined in these measurements and are given in Table 1. The error bar of 2 nm for *h* reflects the height distribution of all the particles. Comparing calcined and reduced samples, the particle height *h* and number density *n* are identical within experimental error. This result indicates that the particle shape is changed after reduction, because the atomic density of Cu in metallic Cu is about two times larger than that in CuO.

Assuming a certain particle shape, we can calculate the mean particle height from the metal loading *l* (from RBS) and particle number density *n* (from AFM), as will be shown below, and we can compare the result with the measured height *h*. Spherical, hemispherical, and intermediate particle shapes are considered.

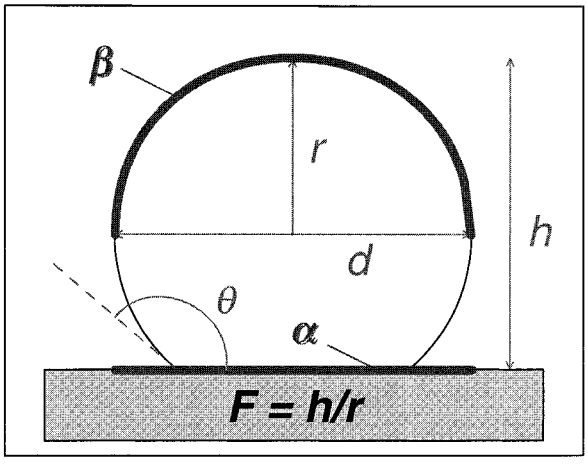

Figure 4. Schematic illustration of a supported particle. The parameters that are involved in models of the particle shape and coverage (see text) are indicated in this picture.

As illustrated in Figure 4, the particle shape can be described by the shape factor *F*:

$$h = F \cdot r \tag{1}$$

where $F = 1$ represents a hemispherical shape and $F = 2$

TABLE 2: Particle Height of Calcined and Reduced Cu Model Catalysts (Samples I, II, III) Calculated (See Text) from the Cu Loading (from RBS) and the Particle Number Density (from AFM) for Several Particle Shapes[a]

	CuO particle height h (nm)				Cu particle height h (nm)			
	$F = 1$ ($\theta = 90°$)	$F = 1.33$ ($\theta = 109°$)	$F = 1.64$ ($\theta = 130°$)	$F = 2$ ($\theta = 180°$)	$F = 1$ ($\theta = 90°$)	$F = 1.33$ ($\theta = 109°$)	$F = 1.64$ ($\theta = 130°$)	$F = 2$ ($\theta = 180°$)
I	9	10	12	14	7	8.5	10	11.5
II	9	10	12	14	7	8.5	9.5	11.5
III	10	12	13.5	16	8.5	10	11	13

[a] The experimental values found for the particle height are shown in Table 1.

TABLE 3: Results of the LEIS Measurements of the Reduced Cu Model Catalysts (Samples I, II, III)[a]

	LEIS	Cu surface coverage (10^{13} at/cm^2)			
	$\frac{S_{Cu}^{Cu\ part.}}{S_{Cu}^{Cu}}$	LEIS A	AFM−RBS A $F = 1$, $\theta = 90°$, coverage = α	AFM−RBS B $F = 1.64$, $\theta = 130°$, coverage = α	AFM−RBS C $F = 1.64$, $\theta = 130°$, coverage = β
I	0.014 ± 0.003	2.5	6	4.5	8.5
II	0.016 ± 0.003	3	6.5	5	10
III	0.022 ± 0.003	4	8	5	9.5

[a] The Cu surface coverage is calculated (see text) using these LEIS results and using AFM−RBS results (from Table 1 and 2).

represents a spherical shape. We do not consider particles with a shape factor $F < 1$, because a combination of AFM and electron microscopy measurements showed that $F \geq 1$ for the particles on the Cu/SiO_2 model catalysts.[6,8,34] The shape factor F is also related to the contact angle θ by:

$$F = 1 - \cos\theta \tag{2}$$

The contact angle θ is a parameter that is often used in wetting/nonwetting studies.[35,36] The volume of a particle (V) depends on the factor F and particle height h:

$$V = \left[\frac{4}{3} - (2 - F)^2 + \frac{1}{3}(2 - F)^3\right] \cdot \frac{\pi}{F^3} \cdot h^3 \quad 1 \leq F \leq 2 \tag{3}$$

The particle volume V can be calculated from l and n in Table 1, assuming that the atomic density of Cu in a particle is equal to ρ^*:

$$V = \frac{l}{n \cdot \rho^*} \tag{4}$$

The atomic density ρ^* (in at/cm^3) is equal to $\rho \cdot N_{AV}/M$, where N_{AV} is the number of Avogadro (6.02×10^{23} at/mol), ρ is the bulk density (in g/cm^3) and M is the molar mass (in g/mol). Then the particle height h can be calculated by inserting the particle volume V obtained from eq 4 in eq 3 and assuming a certain particle shape (F). The results for both CuO and Cu particles are given in Table 2 for different particle shapes.

Let us first consider the CuO particles. The measured particle height of CuO particles (from AFM) is in good agreement with the hemispherical model ($F = 1$). A hemispherical particle shape is also reported in literature for technical CuO/SiO_2 catalysts.[10,37] Electron microscopy measurements of similar Cu model catalysts showed that the CuO particle diameter d is approximately 1.5−2 times the particle height h (from AFM).[6,8,34] If $d/h = 2$, the CuO particles have a hemispherical shape ($F = 1$), confirming the conclusion from RBS and AFM measurements. If $d/h = 1.5$, the CuO particles are more rounded ($F = 1.33$) and make less contact with the substrate ($\theta = 109°$) in comparison with a hemispherical particle ($\theta = 90°$). When we use $F = 1.33$ in our model, the calculated CuO particle height (see Table 2) is still in reasonable agreement with the measured height (see Table 1), within the accuracy of the measurements and the model.

In general, metals in an oxidic state will tend to wet an oxidic substrate, whereas metals in a metallic state will tend to ball up because of their high surface free energy.[16,38,39] It is expected that the (metallic) Cu particles on the reduced model catalysts are more spherical than the particles on the calcined model catalysts. In a transmission electron microscopy (TEM) analysis of technical Cu/SiO_2 catalysts, it was observed that reduction of hemispherical CuO disks in hydrogen produced more rounded metallic Cu particles of somewhat smaller dimensions.[10,37] The contact angle is a good measure for such a wetting/nonwetting phenomenon. For molten Cu droplets on an oxidic substrate, the contact angle is approximately 130°.[40,41]

If we look at the particle height calculated from l and n (Table 2), it is clear that for a given shape the particle height has become smaller after reduction. The observation with UHV-AFM that the particle height does not change after reduction indicates that the reduced Cu particles are more rounded in order to exhibit a particle height similar to that before reduction. However, if we compare the measured particle height of 8 ± 2 nm (Table 1) with the values in Table 2, this ball-up effect cannot be discerned accurately. For the reduced Cu particles, both a model based on hemispherical particles ($F = 1$) and particles having a contact angle of 130° with the support ($F = 1.64$) agree reasonably (within experimental error) with the experimental results.

3.4. Cu Surface Coverage of the Cu/SiO_2 Model Catalyst. To establish the relation between properties and performance of a metal catalyst, it is not only necessary to know the morphology of the catalyst, but also the amount of surface metal atoms/cm^2 (metal surface coverage). A comparison of the performance between catalysts with different properties is only possible if the catalytic activity is normalized to the number of available metal sites (turnover number). LEIS may be useful to determine the Cu surface coverage of the Cu model catalyst. However, LEIS analysis of small supported particles can be complicated by enhanced sputtering of the atoms of the particle,[42] the presence of adsorbates, and by shielding effects related to the surface morphology of the catalyst.[43]

Typical LEIS spectra of the Cu model catalyst are shown in Figure 5a. After reduction, a clear change in Cu signal is visible with respect to the calcined sample, while the oxygen and silicon signals do not change significantly. When 3 keV $^4He^+$ ions are used, LEIS is about 10 times more sensitive for Cu atoms than for Si atoms in our ion scattering experiments. Thus, if the change in Cu signal is related to a change in coverage of the substrate, we do not expect to see a significant change in Si signal (substrate) because of a change in shielding by Cu.

The Cu LEIS signal of the CuO particles ($S_{Cu}^{CuO\ part.}$) is

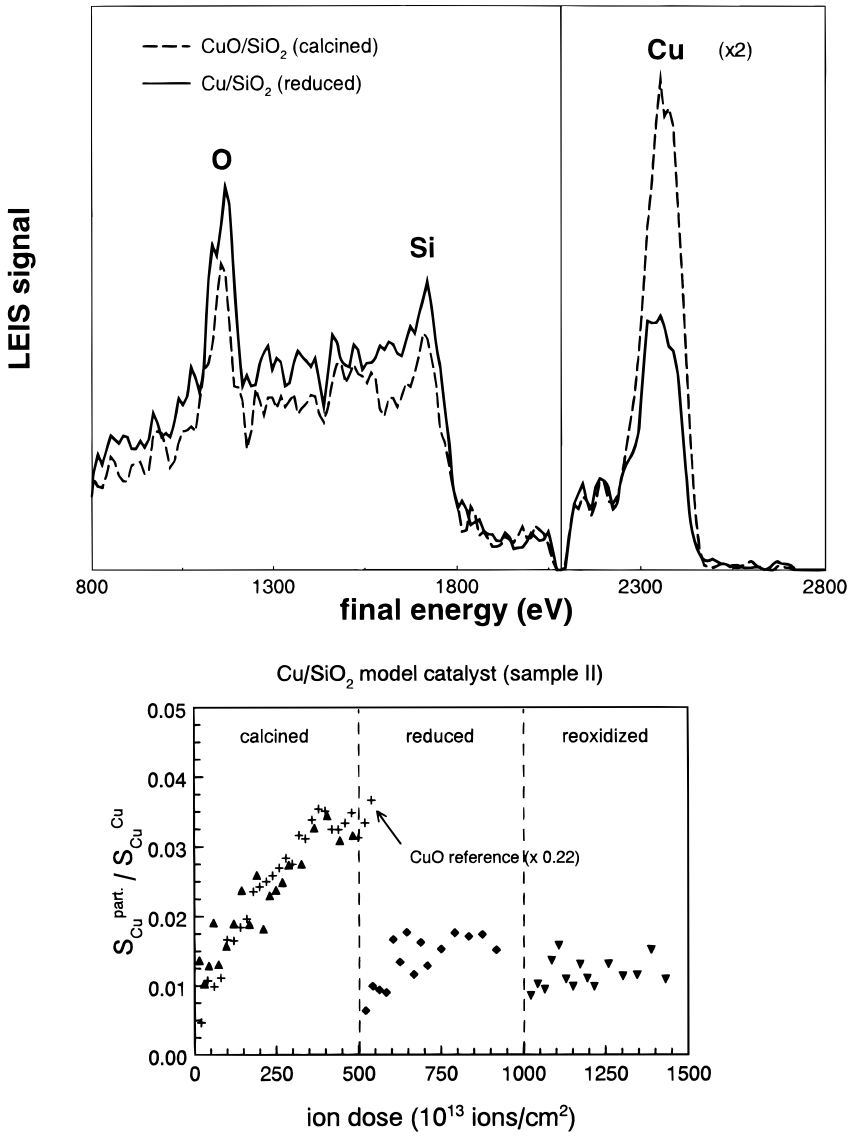

Figure 5. Results of LEIS measurements of a Cu/SiO_2 model catalyst: (a) typical LEIS spectra after calcination and reduction and (b) Cu signals (normalized to the signal of pure Cu) as a function of ion dose after calcination, reduction and reoxidation.

normalized to the Cu signal of a pure Cu sample (S_{Cu}^{Cu}) and was measured as a function of ion dose (see Figure 5b for sample II). The Cu signal of the CuO particles was compared with the Cu signal of bulk polycrystalline CuO (S_{Cu}^{CuO}) in Figure 5b as a function of ion dose and the course of the sputter profiles were found to be the same. The results of the other samples were similar as the results shown in Figure 5b. An additional oxidation step (60 mbar oxygen at 300 °C for 1 h) to burn off surface carbon contaminations did not change the Cu signal of the CuO particles significantly. The increase of the Cu signal of CuO particles as a function of ion dose is attributed to the removal of surface species (containing H and O).[43] The Cu signal of the reduced Cu particles ($S_{Cu}^{Cu\ part.}$) also increases slightly with ion dose. After an ion dose of about 10^{16} He^+/cm^2, no sputter damage of the particles was observed in AFM images.

The normalized Cu signals obtained after an ion dose of 4×10^{15} He^+/cm^2 were used as a measure of the Cu surface coverage of the calcined and reduced model catalysts. Because the Cu signal was initially not constant, we took the Cu signals at a higher ion dose. It was found that the Cu signals of a polycrystalline CuO sample[43] and the particles were constant after an ion dose of about 4×10^{15} He^+/cm^2. For the calcined model catalysts, an estimate of the surface coverage also was made by comparing the Cu signals of the particles with the signal of a polycrystalline CuO sample.

3.4.1. Cu Surface Coverage of the Reduced Model Catalyst. First we will discuss the Cu LEIS signals of the reduced model catalysts. The $S_{Cu}^{Cu\ part.}/S_{Cu}^{Cu}$ ratios after sputtering with about 4×10^{15} He^+/cm^2 are given in Table 3. The surface coverage is determined with LEIS as

$$N_{Cu} = (S_{Cu}^{Cu\ part.}/S_{Cu}^{Cu})\cdot(\rho_{Cu}{}^*)^{2/3}$$

(LEIS model A in Table 3)

assuming that after hydrogen treatment and ion bombardment with about 4×10^{15} He^+/cm^2 the surface of the Cu particles is not covered with adsorbates that shield the Cu surface atoms. The surface coverage can also be estimated independently from the AFM−RBS data by:

$$N_{Cu} = n\cdot\pi r^2\cdot(\rho_{Cu}{}^*)^{2/3}$$

(AFM−RBS models A, B in Table 3)

This is done for a hemispherical particle ($F = 1$, $\theta = 90°$; AFM−RBS model A) and a particle which is more rounded ($F = 1.64$, $\theta = 130°$; AFM−RBS model B), taking the area of the

TABLE 4: Results of the LEIS Measurements of the Calcined Cu Model Catalysts (Samples I, II, III)[a]

	LEIS		Cu surface coverage (10^{13} at/cm^2)		
	$\frac{S_{Cu}{}^{CuO\ part.}}{S_{Cu}{}^{Cu}}$	$\frac{S_{Cu}{}^{CuO\ part.}}{S_{Cu}{}^{CuO}}$	LEIS A	LEIS B	AFM−RBS A $F = 1, \theta = 90°$, coverage = α
I	0.030 ± 0.005	0.23 ± 0.05	6	30	7
II	0.032 ± 0.005	0.22 ± 0.05	6	29	8
III	0.035 ± 0.005	0.25 ± 0.05	7	33	7

[a] The measured Cu signals are normalized to the Cu signal of a pure Cu as well as a CuO reference. The Cu surface coverage is calculated (see text) using these LEIS results and using AFM−RBS results (from Table 1 and 2).

particles projected onto the flat substrate as relevant for the surface coverage and detected by LEIS (indicated by α in Figure 4). The particle number density n is taken from Table 1, the particle radius r is taken from Table 2 using eq 1, and $(\rho_{Cu}{}^*)^{2/3}$ is equal to 1.9×10^{15} Cu at/cm^2. If we take the surface area of the top hemisphere as the relevant parameter for the surface coverage and detected by LEIS (indicated by β in Figure 4), the coverage can be estimated by

$$N_{Cu} = n \cdot 2\pi r^2 \cdot (\rho_{Cu}{}^*)^{2/3}$$

(AFM−RBS model C in Table 3)

This is done for more spherical particles ($F = 1.64$, $\theta = 130°$).

Table 3 presents the results of all the models described above. If we make a comparison between the LEIS and AFM−RBS models, LEIS model A is in reasonable agreement with AFM−RBS model B. These experiments indicate that the reduced Cu particles have a shape that is more rounded than hemispherical, as was also discussed in section 3.3. We also note that the Cu surface coverage as detected by LEIS corresponds approximately with the projected surface area of the Cu particles (model α in Figure 4), which contains a lower number of Cu atoms than that present at the surface of the particles. Most probably the Cu atoms at the surface of the particles are not completely visible in our LEIS experiments because of shielding effects by neighboring atoms.[43]

3.4.2 Cu Surface Coverage of the Calcined Model Catalyst. The Cu surface coverage of the calcined model catalysts has been studied in a way similar to that for the reduced model catalysts. In Table 4, the $S_{Cu}{}^{CuO\ part.}/S_{Cu}{}^{Cu}$ ratios after an ion dose of about 4×10^{15} He^+/cm^2 and the $S_{Cu}{}^{CuO\ part.}/S_{Cu}{}^{CuO}$ ratios (which do not depend on ion dose as shown in Figure 5b) of the calcined model catalysts are shown. Using these ratios, a Cu surface coverage can be determined as

$$N_{Cu} = (S_{Cu}{}^{CuO\ part.}/S_{Cu}{}^{Cu}) \cdot (\rho_{Cu}{}^*)^{2/3}$$

(LEIS model A in Table 4)

or it can be estimated by

$$N_{Cu} = (S_{Cu}{}^{CuO\ part.}/S_{Cu}{}^{CuO}) \cdot (\rho_{CuO}{}^*)^{2/3}$$

(LEIS model B in Table 4)

The difference between these two models is that no shielding of Cu by oxygen in the ion scattering event is assumed in LEIS model A, whereas in LEIS model B shielding of Cu by oxygen occurs and is the same for the Cu surface atoms of CuO particles and bulk CuO (reducing the Cu signal by a factor of 5−6, see also ref 43). The Cu surface density in CuO $(\rho_{CuO}{}^*)^{2/3}$ is equal to 1.3×10^{15} Cu at/cm^2. An estimate of the surface coverage from AFM−RBS data is made using

$$N_{Cu} = n \cdot \pi r^2 \cdot (\rho_{CuO}{}^*)^{2/3}$$

(AFM−RBS model A in Table 4)

This is done for a hemispherical particle ($F = 1$, $\theta = 90°$). The area of the particles projected onto the substrate (model α in Figure 4) is taken as the relevant parameter for the surface coverage in a comparison between the AFM−RBS model and the LEIS models, because the better agreement with LEIS results was found for the metallic Cu particles using this assumption (see Table 3).

Although we expect that LEIS model B, including the correction for shielding of Cu atoms by oxygen atoms, is the best LEIS model to determine the Cu surface coverage of the calcined model catalysts, values from AFM−RBS model A are much lower than from LEIS model B and in good agreement with LEIS model A. If an AFM−RBS model with another particle shape is considered ($F > 1$), the difference between this AFM−RBS model and LEIS model B becomes even larger. We will discuss three possible explanations for these results.

A first explanation is that Cu atoms may be less shielded by oxygen (and, therefore, much more visible with LEIS) at the surface of the calcined Cu model catalyst than at the surface of bulk polycrystalline CuO. We do not know the values of the shielding factor for both systems,[43] but the difference in the shielding factor would be rather large to explain our results.

A second possibility is that the Cu surface density of the CuO particles is higher than that of bulk CuO. Preferential exposure of surface planes in small supported particles can result in a different metal surface density for particles compared to the metal surface density of the bulk material.[44,45] However, we do not expect that this difference can be as large as that observed here and we assume that the close-packed (111) plane is dominant on the polycrystalline CuO surface.

The third possibility is that more Cu surface atoms are present than expected from the AFM−RBS data. The amount that is "invisible" for AFM and too small to affect RBS results would be $20-25 \times 10^{13}$ Cu at/cm^2 when LEIS model B is compared with AFM−RBS model A. If these Cu atoms are highly dispersed over the SiO_2 substrate, these species will not be visible with AFM and are approximately within the experimental error of the RBS measurements. If these Cu species are atomically dispersed, the density is 2−2.5 Cu at/nm^2 and this corresponds with the amount of Si−OH groups that is expected to be present at the surface of our model supports.[21−24] The atomically dispersed Cu species may be attached to these silanol groups during spin-coating and/or calcination. The observation of a low particle number density (from AFM) in combination with a high Cu loading (from RBS) after calcination to 450 °C at a low ramp rate of 50 °C/h, as mentioned in section 3.2, can be understood by assuming the formation of these highly dispersed Cu species to a larger extent.

During reduction, the highly dispersed Cu species migrate to the 8 nm Cu particles and/or form new particles, because mainly 8 nm particles are left after reduction as indicated by the results of the AFM−RBS measurements compared to the LEIS measurements (see Tables 1, 2, and 3). Upon reoxidation of the reduced model catalyst in 50 mbar O_2 at 300 °C for 1 h, the Cu LEIS signal does not change significantly (see Figure 5b), indicating that the migration process cannot be easily reversed by this treatment.

XPS measurements also indicated that the dispersion changed significantly upon reduction: the Cu(2p)/Si(2p) intensity ratio decreased by a factor of 1.7, when a calcined and reduced Cu/SiO_2 model catalyst were compared. A rough estimate can be

made of the change in XPS intensity ratio by using a simple layer model with the layer thickness and coverage as parameters.[46] A Cu layer with a thickness of 8 nm and a coverage of 2% of the support was chosen as a model for the reduced samples. A combination of a CuO layer (thickness = 8 nm, coverage = 3%) and a CuO monolayer (thickness = 0.3 nm, coverage = 20%) was chosen as a model for the calcined samples, based on the results presented above. For this case, we have calculated that the Cu(2p) XPS intensity decreases upon reduction by a factor of 2.3, which is of the same order as that found experimentally. This result gives more evidence for the proposed structure of the Cu model catalysts.

4. Structure of the Cu/SiO_2 Model Catalyst. The structure of the wet-chemically prepared Cu/SiO_2 model catalyst can be characterized in detail after each preparation step. Two types of Cu species are present at the surface of the calcined Cu model catalyst: hemispherical CuO particles (with a particle height of about 8 nm) and Cu species highly dispersed over the SiO_2 substrate. Upon reduction in hydrogen, metallic Cu particles are formed both by reduction of the CuO particles and by migration and/or agglomeration of the highly dispersed Cu species. The metallic Cu particles have the same particle height as the CuO particles, but are most probably more spherical.

We will compare this structure of the Cu/SiO_2 model catalysts with the structure of technical Cu/SiO_2 catalysts. Catalysts of Cant et al.[10,37] were prepared by the equilibration of nonporous aerosil spheres with an excess of a Cu tetraamine solution, followed by washing and calcination in air at 500 °C. The presence of two different Cu species, as observed for the calcined model catalyst, was also found for these technical catalysts. During wet-chemical preparation of the technical catalysts, two processes took place. Ion exchange occured, resulting in the anchoring of the Cu precursor to silanol groups in a well-dispersed form. Precipitation of Cu hydroxide occured, resulting in small particles. Upon calcination of the technical catalysts, Cu was present both as Cu^{2+} ions highly dispersed over the support and as CuO hemispherical disks. Upon reduction in hydrogen at 250−300 °C, isolated ion-exchanged species were reduced to Cu^+, and the CuO particles were reduced to more spherical metallic Cu particles.[10,37] Marchi et al.[11] studied a commercial shell-type Cu/SiO_2 catalyst and also suggested the existance of two different CuO species.

The dispersion of the technical Cu/SiO_2 catalyst of Cant et al. was altered after reduction, as indicated by a decrease in the Cu/Si atomic ratio (from XPS).[37] Migration and agglomeration of the dispersed Cu species may occur. We also suggested such a migration process for the Cu model catalysts during reduction. LEIS experiments after reoxidation of the reduced model catalyst indicate that the migration process cannot be easily reversed by this treatment. This was also found for the technical Cu catalyst of Cant et al.:[37] reoxidation of the reduced catalyst did not result in redispersion of oxidized Cu, because the Cu/Si XPS ratio did not change significantly.

In contrast to the observations on the Cu model catalyst, Cant et al.[10,37] reported that after reduction isolated ion-exchanged Cu species are still present as Cu^+ species because of the strong interaction with the support. No clear contribution of Cu^+ in the XPS spectra could be found after reduction of the Cu model catalysts, indicating that (almost) no highly dispersed Cu species are left on the surface of the reduced model catalysts.

The interaction between Cu and the SiO_2 support strongly influences the processes that change the structure of the catalyst. In a study presented in an accompanying paper,[17] the Cu/SiO_2 model catalysts are used to investigate these metal-support interactions in detail. It will be shown that model catalysts are very helpful when used to study surface and interface phenomena that are determined by the physicochemical interactions between metal and support. Well-defined model catalysts, as presented in this paper, can also be of great help when used to elucidate the active site(s) by testing the model catalysts in catalytic reactions.

5. Conclusion

The wet-chemical approach of making model catalysts involving spin-coating, calcination, and reduction leads to a succesful preparation of realistic Cu/SiO_2 model catalysts. The structure of the wet-chemically prepared Cu/SiO_2 model catalyst can be characterized in detail after each preparation step, concerning the particle size and shape, particle number density, metal surface coverage, total metal loading, and oxidation state of the particles by using UHV−AFM, electron microscopy, LEIS, XPS, and RBS. A combination of characterization techniques is required to characterize this system extensively and to ensure a correct interpretation of the data.

Acknowledgment. We are grateful to Dr. Edgar Kuipers (SRTCA) for helpful discussions and for providing Cu model catalysts and electron microscopy data in the initial stage of our research. We thank Ir. Ronald van den Oetelaar for performing AFM measurements, Dr. Leo van IJzendoorn (Cyclotron, Faculty of Physics, Eindhoven University of Technology) for performing RBS measurements, and Dr. Hans Niemantsverdriet (laboratory for inorganic chemistry and catalysis, Faculty of Chemical Engineering, Eindhoven University of Technology) for the use of his XPS system. The investigations described in this paper were supported by the Netherlands Technology Foundation (STW).

References and Notes

(1) Gunter, P. L. J.; Niemantsverdriet, J. W.; Ribeiro, F. H.; Somorjai, G. A. *Catal. Rev.—Sci. Eng.* **1997**, *38*, 77.
(2) Kuipers, E. W.; Laszlo, C.; Wieldraaijer, W. *Catal. Lett.* **1993**, *17*, 71.
(3) Kuipers, E. W.; Doornkamp, C.; Wieldraaijer, W.; van den Berg, R. E. *Chem. Mater.* **1993**, *5*, 1367.
(4) Doornkamp, C.; Laszlo, C.; Wieldraaijer, W.; Kuipers, E. W. *J. Mater. Res.* **1995**, *10*, 411.
(5) van Hardeveld, R. M.; Gunter, P. L. J.; van IJzendoorn, L. J.; Wieldraaijer, W.; Kuipers, E. W.; Niemantsverdriet, J. W. *Appl. Surf Sci.* **1995**, *84*, 339.
(6) van Wijk, R. *Preparation, stability and reactivity of Cu particles supported on oxidised Si(100)*, Ph.D. Thesis, University of Utrecht, The Netherlands, 1996.
(7) Partridge, A.; Toussaint, S. L. G.; Flipse, C. F. J.; Kuipers, E. W. In *Forces in scanning probe methods;* Guntherodt, H.-J., Anselmetti D., Meyer, E., Eds.; NATO ASI Series E; Kluwer: Dordrecht, 1994; Vol. 286, p 531.
(8) Partridge, A.; Toussaint, S. L. G.; Flipse, C. F. J.; van IJzendoorn, L. J.; van den Oetelaar, L. C. A. *J. Vac. Sci. Technol.* **1996**, *B14*, 585.
(9) Partridge, A.; Toussaint, S. L. G.; Flipse, C. F. J. *Appl. Surf. Sci.* **1996**, *103*, 127.
(10) Cant, N. W.; Sexton, B.; Trimm, D. L.; Wainwright, M. S. In *Surface science: principles and applications*; Howe, R. F.; Lamb R. N.; Wandelt, K., Eds.; Springer Proceedings in Physics; Springer-Verlag: Heidelberg, 1993; Vol. 73, p 290.
(11) Marchi, A. J.; Fierro, J. L. G.; Santamaria, J.; Monzón, A. *Appl. Catal.* **1996**, *A142*, 375.
(12) Klier, K. *Adv. Catal.* **1982**, *31*, 243.
(13) Waugh, K. C. *Catal. Today* **1993**, *18*, 147.
(14) Nonneman, L. E. Y.; Ponec, V. *Catal. Lett.* **1990**, *7*, 213.
(15) Brands, D. S.; Poels, E. K.; Krieger, T. A.; Makarova, O. V.; Weber, C.; Veer, S.; Bliek, A. *Catal. Lett.* **1996**, *36*, 175.
(16) Clausen, B. S.; Schiøtz, J.; Gråbaek, L.; Ovesen, C. V.; Jacobsen, K. W.; Nørskov, J. K.; Topsøe, H. *Topics Catal.* **1994**, *1*, 367.
(17) van den Oetelaar, L. C. A.; Partridge, A.; Toussaint, S. L. G.; Flipse, C. F. J.; Brongersma, H. H. *J. Phys. Chem. B* **1998**, *102*, 9541.

(18) de Jong, A. M. Surface spectroscopy of model catalysts. Ph.D. Thesis, Eindhoven University of Technology, The Netherlands, 1994.
(19) Grunthaner, F. J.; Grunthaner, P. J.; Vasquez, R. P.; Lewis, B. F.; Maserjian, J.; Madhukar, A. *Phys. Rev. Lett.* **1979**, *43*, 1683.
(20) Hollinger, G.; Himpsel, F. J. *J. Vac. Sci. Technol.* **1983**, *A1*, 640.
(21) Boehm, H. P. *Adv. Catal.* **1966**, *16*, 179.
(22) Iler, R. K. *The chemistry of silica: solubility, polymerization, colloid and surface properties, and biochemistry*; John Wiley and Sons: Chichester, 1979.
(23) Zhuravlev, L. T. *Langmuir* **1987**, *3*, 316.
(24) Bergna, H. E. In *The colloid chemistry of silica;* Bergna, H. E., Ed.; Advances in Chemistry Series; American Chemical Society: Washington, 1994; Vol. 234, p 1.
(25) Nanoscope, Digital Instruments, 520 E. Montecito St., Santa Barbara, CA.
(26) Mahoney, W.; Schaefer, D. M.; Patil, A.; Andres, R. P.; Reifenberger, R. *Surf Sci.* **1994**, *316*, 383.
(27) Brongersma, H. H.; Hazewindus, N.; van Nieuwland, J. M.; Otten, A. M. M.; Smets, A. J. *Rev. Sci. Instrum.* **1978**, *49*, 707.
(28) van IJzendoorn, L. J.; Niemantsverdriet, J. W.; Severens, R. J.; van Dijk, P. W. L.; de Voigt, M. J. A. *Nucl. Instrum. Methods* **1994**, *B89*, 114.
(29) van Wijk, R.; Gijzeman, O. L. J.; Geus, J. W.; ten Grotenhuis, E.; van Miltenburg, J. C. *Catal. Lett.* **1994**, *24*, 171.
(30) ten Grotenhuis, E.; van Miltenburg, J. C.; van der Eerden, J. P.; van Wijk, R.; Gijzeman, O. L. J.; Geus, J. W., Marée, C. H. M. *Catal. Lett.* **1994**, *28*, 109.
(31) Fleisch, T. H.; Mieville, R. L. *J. Catal.* **1984**, *90*, 165.
(32) Peplinski, B.; Unger, W. E. S.; Grohmann, I. *Appl. Surf. Sci.* **1992**, *62*, 115.
(33) Che, M.; Bennet, C.O. *Adv. Catal.* **1989**, *36*, 55.
(34) Reijerse, J. F. C.-J. M. *Particle morphology from XPS data: design and implementation of a quantification procedure for nanoscale metal particles*; Stan Ackermans Instituut: Eindhoven, 1995.
(35) Zisman, W. A. In *Contact angle, wettability, and adhesion*; Gould, R. F., Ed.; Advances in Chemistry Series; American Chemical Society: Washington, 1964; Vol. 43, p 1.
(36) de Gennes, P. G. *Rev. Mod. Phys.* **1985**, *57*, 827.
(37) Kohler, M. A.; Curry-Hyde, H. E.; Hughes, A. E.; Sexton, B. A.; Cant, N. W. *J. Catal.* **1987**, *108*, 323.
(38) Pretorius, R.; Harris, J. M.; Nicolet, M.-A. *Solid-State Electronics* **1978**, *21*, 667.
(39) Diebold, U.; Pan, J.-M.; Madey, T. E. *Surf Sci.* **1994**, *331−333*, 845.
(40) Eustathopoulos, N.; Chatain, D.; Coudurier, L. *Mater. Sci. Eng.* **1991**, *A135*, 83.
(41) Cannon, R. M.; Saiz, E.; Tomsia, A. P.; Carter, W. C. *Mat. Res. Soc. Symp. Proc.* **1995**, *357*, 279.
(42) den Otter, W. K.; Brongersma, H. H.; Feil, H. *Surf. Sci.* **1994**, *306*, 215.
(43) van den Oetelaar, L. C. A.; van Benthem, H. E.; Helwegen, J. H. J. M.; Stapel, P. J. A.; Brongersma, H. H. *Surf. Interface Anal.* **1998**, *26*, 537.
(44) Sundquist, B. E. *Acta Metallurgica* **1964**, *12*, 67.
(45) Schmidt, L. D.; Lee, C.-P. In *Catalyst deactivation;* Petersen, E. E., Bell, A. T., Eds.; Chemical Industries; Marcel Dekker: New York, 1987; Vol. 30, p 297.
(46) Borg, H. J.; van den Oetelaar, L.C.A.; van IJzendoorn, L. J.; Niemantsverdriet, J. W. *J. Vac. Sci. Technol.* **1992**, *A10*, 2737.